PHYSICAL REVIEW A VOLUME 26, NUMBER 4 OCTOBER 1982

Collective effects on the operation of free-electron lasers with an axial guide field

H. P. Freund* and P. Sprangle
Naval Research Laboratory, Washington, D.C. 20375

D. Dillenburg, E. H. da Jornada, R. S. Schneider, and B. Liberman
Instituto de Fisica, Universidade Federal do Rio Grande do Sul, 90.000 Porto Alegre-RS, Brazil
(Received 14 December 1981)

The collective interaction in a free-electron laser with combined helical wiggler and uniform axial guide fields is presented in the linearized regime. The analysis involves a perturbation of the Vlasov-Maxwell equations about the constant-velocity helical trajectories, and the general driving currents are derived for this configuration. The complete dispersion equation is then obtained for a monoenergetic beam. Analytic solutions are obtained in the strong pump and space-charge dominated regimes, and an extensive numerical analysis is presented for a wide range of operating parameters. The results indicate that substantial enhancements in the gain are possible when the relativistic axial gyrofrequency is comparable to the free-electron laser doppler upshift. In addition, there is a range of parameters for which the ponderomotive potential acts to destabilize the electron beam. In this regime, we find both unstable electrostatic beam modes and largely electromagnetic modes with broad bandwidths.

I. INTRODUCTION

The physical process which gives rise to wave amplification in free-electron lasers stems from the interaction of a relativistic electron beam with a spatially periodic magnetic field (i.e., the wiggler or pump field) applied largely transverse to the direction of bulk electron motion. The effect of the wiggler field is to provide a coupling between the electron beam and electromagnetic radiation fields which results in a ponderomotive force along the axis of the beam. The form of the interaction can be classified in a variety of ways depending upon such parameters as the magnitude of the electron current, the strength of the pump field, the bulk energy and energy spread of the beam, and the length of the interaction region. For example, on the one hand, thermal effects can be neglected when the energy spread in the beam $\Delta E \ll E_0/N$, where E_0 is the bulk beam energy and N is the number of wiggler periods in the interaction region. In this regime the entire electron beam participates in the interaction; however, collective (i.e., electrostatic) effects are important only when the fluctuating space-charge potential is comparable to the ponderomotive potential. The interaction in this collective regime is referred to as stimulated Raman scattering, and describes the coupling of a negative-energy space-charge wave and a positive-energy electromagnetic wave through the presence of the wiggler. On the other hand, when thermal effects are important, the radiation is resonant with only a small fraction of the beam and the process is termed stimulated Compton scattering. We shall be concerned in this paper with the cold-beam limit, and deal with both the single-particle and collective regimes.

An additional factor in the interaction is introduced by practical limitations in the propagation of intense electron beams; specifically, that an axial guide field is required to collimate intense beams in the transverse direction. This is of primary importance to free-electron laser experiments operating at millimeter wavelengths[1-5] which employ relatively high-current ($\gtrsim 1$ kA) and low-energy (~ 1 MeV) electron beams. In contrast, an axial guide field is not a practical necessity for infrared free-electron laser experiments[6-8] which typically operate at much lower ambient currents (~ 1 A) but higher energies (~ 50 MeV). However, the effect of the axial guide field on the free-electron laser mechanism may be relevant in the latter case as well because of enhancements in the gain which may result when a guide field is present.

The effects of an axial guide field have been treated from the standpoints of both a fluid[9-13] and a kinetic[14-16] theory. It is our purpose in this work to treat the question of the free-electron laser instability in the presence of an axial guide field in both the tenuous (i.e., single-particle regime) and dense

(i.e., Raman regime) beam limits by means of a solution of the Vlasov-Maxwell equations. In the interest of analytic tractability a cold-beam approximation is imposed, and the contributions due to cyclotron mode interactions are included. The organization of the paper is as follows. In Sec. II, we develop the fluctuating source currents by solution of the Vlasov equation. The unperturbed orbits are assumed to be constant axial velocity (helical) trajectories,[17,18] and the source currents are found for a general equilibrium distribution. The general dispersion equation is obtained in Sec. III, and solved in several analytically accessible regimes for a cold-beam limit. A detailed numerical solution is presented in Sec. IV for a wide range of operating parameters. A summary and discussion appears in Sec. V.

II. THE SOURCE CURRENT

In this section we derive the fluctuating source current by means of solution of the linearized Vlasov equation. The physical configuration we consider is that of a relativistic electron beam propagating through an ambient magnetic field composed of a periodic helical wiggler field and a uniform axial guide field

$$\vec{B}=B_0\hat{e}_z+\vec{B}_w(r,z)\ , \tag{1}$$

where the wiggler field is assumed to be generated with a bifilar helix and is derived from a vector potential of the form[19]

$$\vec{A}_w=-\frac{2B_w}{k_w}\left[\frac{1}{k_w r}I_1(k_w r)\cos(\theta-k_w z)\hat{e}_r - I_1'(k_w r)\sin(\theta-k_w z)\hat{e}_\theta\right] \tag{2}$$

in cylindrical coordinates. In Eq. (2), B_w and k_w ($\equiv 2\pi/\lambda_w$, where λ_w is the wiggler period) are assumed to be constant and I_1 and I_1' are the modified Bessel function of the first kind and its derivative, respectively. Since for most free-electron laser experiments the initial beam radius is a small fraction of the wiggler period, we shall expand in powers of $k_w r$ and write

$$\vec{B}_w\simeq B_w(\hat{e}_x\cos k_w z+\hat{e}_y\sin k_w z)\ . \tag{3}$$

The single-particle orbits in these combined fields have been amply discussed in the literature.[17,18] and will not be discussed in depth here. We shall restrict consideration to orbits which are given approximately by stable helical trajectories, and write[15,18]

$$\begin{aligned} p_x&=\gamma m v_w\cos k_w z+P_x\cos\Omega_0 t-P_y\sin\Omega_0 t\ ,\\ p_y&=\gamma m v_w\sin k_w z+P_x\sin\Omega_0 t+P_y\cos\Omega_0 t\ ,\\ p_z&=\gamma m v_{||}-\beta_w[P_x\cos(k_w z-\Omega_0 t)\\ &\quad -P_y\sin(k_w z-\Omega_0 t)]\ , \end{aligned} \tag{4}$$

where $v_w\equiv\Omega_w v_{||}/(\Omega_0-k_w v_{||})$ and $v_{||}$ are the transverse and axial velocities corresponding to the helical trajectories, $\Omega_{0,w}\equiv|eB_{0,w}/\gamma mc|$, $\gamma\equiv(1-v^2/c^2)^{-1/2}$, $\beta_w\equiv v_w/v_{||}$ is the pump strength parameter, and P_x and P_y are constants which correspond to the canonical momenta in the limit as $B_0\to 0$. Equations (4) are valid as long as $|\beta_w P_{x,y}|\ll|\gamma m v_{||}|$ and require that v_w and $v_{||}$ are related via

$$v_{||}^2+v_w^2=(1-\gamma^{-2})c^2\ , \tag{5}$$

which constitutes a quartic equation for $v_{||}$. Equation (5) describes at most four distinct classes of trajectories, of which one is characterized by motion antiparallel to $\vec{B}_0$ and will be ignored. Of the remaining trajectories having motion parallel to $\vec{B}_0$, we restrict consideration to those which are stable,[17,18] i.e., for which

$$(k_w v_{||}-\Omega_0)[k_w v_{||}-(1+\beta_w^2)\Omega_0]>0\ . \tag{6}$$

The typical dependence of the axial velocity on B_0 is shown in Fig. 1, in which we plot $\beta_{||}$ ($\equiv v_{||}/c$) versus β_0 ($\equiv\Omega_0/k_w c$) for a kinetic energy of 1.5 MeV and wiggler amplitude and period such that $\Omega_w/k_w c=0.05$. There are two classes of stable orbits. One class (referred to as group I) of orbits is

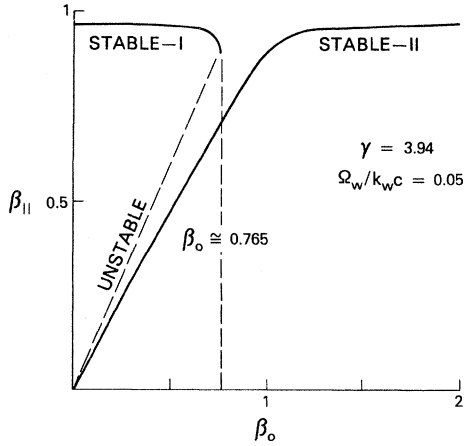

FIG. 1. Graph of the axial velocity vs β_0 ($\equiv\Omega_0/k_w c$) for a beam energy of 1.5 MeV and a wiggler amplitude and period such that $\Omega_w/k_w c=0.05$.

characterized by high axial velocities and has $k_w v_{||} > (1+\beta_w^2)\Omega_0$. For these trajectories the axial velocity decreases monotonically with increasing B_0 until $v_{||} = (1+\beta_w^2)\beta_0 c$ which is the orbital stability boundary. For the parameters shown, this occurs for $\beta_0 \simeq 0.765$. The second class of orbits (group II) is characterized by an axial velocity which increases monotonically from zero with increasing B_0, and high axial velocities are, typically, found only when $\beta_0 \gtrsim 1$. In contrast to group I trajectories, the stability criterion (6) is satisfied for these orbits because $k_w v_{||} < \Omega_0$. It will be shown in Sec. III that the relative magnitude of $k_w v_{||}$ and Ω_0 for group I and II orbits has important consequences on the excited spectrum. Finally, it is important to note that $k_w v_{||} \neq \Omega_0$ for either class of orbits. Were the equality to hold it would imply an infinite v_w which would violate the conservation of energy represented by Eq. (5).

The source current is obtained from the velocity moments of the perturbed distribution function $\delta f_b(z,\vec{p},t) = f_b(z,\vec{p},t) - F_b(p_x,P_y,p)$, where f_b is the complete distribution, F_b is the equilibrium distribution, and δf_b is assumed to be first order in the radiation fields. The formal solution of the Vlasov equation to this order is

$$\delta f_b(z,\vec{p},t(z)) = e\int_0^z \frac{dz'}{v_z(z')}\left[\delta\vec{E}(z',t(z)) + \frac{1}{c}\vec{v}(z')\times\delta\vec{B}(z',t(z'))\right]\frac{\partial F_b}{\partial\vec{p}(z')}\ , \tag{7}$$

where the solution is parametrized in terms of the axial position relative to the start of the interaction region (at $z=0$) and $t(z) = t_0 + \int_0^z dz'/v_z(z')$ is the sum of the time required for an electron to transverse the distance z and the entry time t_0.

We assume plane-wave solutions of the form $\exp(-i\omega t)$ and choose to work with the scalar and vector potentials

$$\delta\phi(z,t) = \tfrac{1}{2}\delta\hat{\phi}(z)\exp(-i\omega t) + \text{c.c.}$$

and

$$\delta\vec{A}(z,t) = \tfrac{1}{2}\delta\hat{A}(z)\exp(-i\omega t) + \text{c.c.}\ ,$$

where $\hat{e}_z\cdot\delta\hat{A}(z) = 0$. In addition, since the assumption of small P_x and P_y are implicit in the analysis, we adopt an equilibrium distribution of the form

$$F_b(P_x,P_y,p) = n_b\delta(P_x)\delta(P_y)G_b(p)\ , \tag{8}$$

where n_b is the number density of the beam, and $G_b(p)$ is an arbitrary function subject to the normalization condition $\int_0^\infty dp\, pG_p(p)/p_z = 1$. Observe that the choice of a distribution of this form (8) confines the equilibrium trajectories to be those constant axial velocity (helical) orbits described by (5). The interested reader is referred to Freund *et al.*[15] for a detailed derivation of the perturbed distribution and source current. We confine ourselves here to the final result. With respect to the basis $\hat{e}_\pm = \frac{1}{2}(\hat{e}_x \pm i\hat{e}_y)$, the source current can be written in the form

$$\delta\vec{J}(z,t) = [\delta\hat{J}_+(z)\hat{e}_+ + \delta\hat{J}_-(z)\hat{e}_- + \delta\hat{J}_z(z)\hat{e}_z]\exp(-i\omega t) + \text{c.c.}\ , \tag{9}$$

where

$$\delta\vec{J}_\pm(z) = \frac{\omega_b^2}{8\pi c}\int_0^\infty dp\frac{p}{\gamma p_z}\left[\exp[\mp i\Omega_0 t(z)]\left[2+\frac{p_+p_-}{p_z^2}\right]D_\pm + \exp[\pm i\Omega_0 t(z)]\frac{p_\pm^2}{p_z^2}D_\mp \right.$$
$$\left. + p_\pm\left[\frac{\partial}{\partial P_x} + i\frac{\partial}{\partial P_y}\right]D_+ + p_\pm\left[\frac{\partial}{\partial P_x} - i\frac{\partial}{\partial P_y}\right]D_- - p_\pm D_z\frac{\partial}{\partial p}\right]G_b(p)\Big|_{P_x=P_y=0} \tag{10}$$

and

$$\delta\hat{J}_z(z) = \frac{\omega_b^2}{8\pi c}\int_0^\infty dp\frac{p}{\gamma}\left[\left[\frac{\partial}{\partial P_x} + i\frac{\partial}{\partial P_y}\right]D_+ + \left[\frac{\partial}{\partial P_x} - i\frac{\partial}{\partial P_y}\right]D_- - D_z\frac{\partial}{\partial p}\right]G_b(p)\Big|_{P_x=P_y=0}\ . \tag{11}$$

In Eqs. (10) and (11), ω_b is the beam plasma frequency, $p_\pm \equiv p_x \mp i p_y$,

$$D_\pm \equiv -\exp[\pm i\Omega_0 t(z)]\{\delta\hat{A}_\pm(z)-\delta\hat{A}_\pm(0)\exp[i(\omega\mp\Omega_0)\tau(z,0)] \mp i\Omega_0\int_0^z \frac{dz'}{v_z(z')}\delta\hat{A}_\pm(z')\exp[i(\omega\mp\Omega_0)\tau(z,z')]\}\ , \tag{12}$$

and

$$D_z \equiv \frac{\gamma mc}{p}\int_0^z dz'\exp[i\omega\tau(z,z')]\left[-\partial_{z'}\delta\hat{\phi}(z')+\frac{i\omega}{c}\left[\frac{p_-}{p_z}\delta\hat{A}_+(z')+\frac{p_+}{p_z}\delta\hat{A}_-(z')\right]\right]\ , \tag{13}$$

where $\tau(z,z')\equiv t(z)-t(z')$. Finally, we assume the spatial dependence of the fields to be

$$\delta\hat{A}_\pm(z)=\delta\hat{A}_\pm(0)\exp(ik_\pm z)$$

and

$$\delta\hat{\phi}(z)=\delta\hat{\phi}(0)\exp(ikz)\ .$$

As a result, the source currents can be expresed as

$$\delta\hat{J}_\pm(z)=-\frac{\omega_b^2}{8\pi c}\delta\hat{A}_\pm(z)\left[2\left\langle\frac{p}{\gamma p_z}\frac{\omega-k_\pm v_z}{\omega\mp\Omega_0-k_\pm v_{||}}\right\rangle+a_w^2 S_\pm(k_\pm,\omega)\right]-a_w\frac{ck^2}{8\pi}\delta\hat{\phi}(z)e^{\mp ik_w z}\chi_a(k,\omega) \tag{14}$$

and

$$\delta\hat{J}_z(z)=-\frac{\omega k}{8\pi}\delta\hat{\phi}(z)\chi(k,\omega)-\frac{\omega k_w}{8\pi}a_w[\delta\hat{A}_+(z)\exp(ik_w z)\sigma_+(k_+,\omega)+\delta\hat{A}_-(z)\exp(-ik_w z)\sigma_-(k_-,\omega)]\ , \tag{15}$$

where $a_w\equiv eA_w/mc^2$, $\langle(\cdots)\rangle\equiv\int_0^\infty dp\,G_b(p)(\cdots)$,

$$\chi(k,\omega)\equiv\frac{\omega_b^2}{k}\int_0^\infty dp\frac{m}{\omega-kv_{||}}\frac{\partial G_b}{\partial p}\ , \tag{16}$$

$$\chi_a(k,\omega)\equiv\frac{\omega_b^2}{k}\int_0^\infty dp\frac{k_w v_{||}}{k_w v_{||}-\Omega_0}\frac{m}{\gamma(\omega-kv_{||})}\frac{\partial G_b}{\partial p}\ , \tag{17}$$

$$S_\pm(k_\pm,\omega)\equiv\int_0^\infty dp\frac{p}{\gamma^3 p_{||}}G_0(p)\frac{c^2k_w^2}{(k_w v_{||}-\Omega_0)^2}\left[1+\frac{\Omega_0}{k_w v_{||}-\Omega_0}\left[\frac{\omega\mp\Omega_0\pm k_w v_{||}}{\omega\mp\Omega_0-kv_{||}}-\frac{\omega\mp k_w v_{||}}{\omega\mp k_w v_{||}-k_\pm v_{||}}\right]\right] -\omega c^2\int_0^\infty dp\frac{k_w^2 v_{||}}{\gamma^2(k_w v_{||}-\Omega_0)^2}\frac{m}{\omega\mp k_w v_{||}-k_\pm v_{||}}\frac{\partial G_p}{\partial p}\ , \tag{18}$$

$$\sigma_\pm(k_\pm,\omega)\equiv\frac{\omega_b^2}{\omega}\int_0^\infty dp\left[\frac{\omega}{\gamma(k_w v_{||}-\Omega_0)}\frac{mv_{||}}{\omega\mp k_w v_{||}-k_\pm v_{||}}\frac{\partial}{\partial p} +\frac{p}{\gamma^2 p_{||}}\frac{\Omega_0}{(k_w v_{||}-\Omega_0)^2}\left[\frac{\omega\mp k_w v_{||}}{\omega\mp k_w v_{||}-k_\pm v_{||}}-\frac{\omega}{\omega\mp\Omega_0-k_\pm v_{||}}\right]\right]G_b(p)\ , \tag{19}$$

and it has been assumed that $G_b(p)=0$ for $p=0,\ \infty$. Observe that Eqs. (14)–(19) are equivalent to the result found by Sprangle and Smith[20] in the limit as $B_0\to 0$.

III. THE DISPERSION EQUATION

The dispersion equation is obtained by substitution of the source currents [Eqs. (14)–(19)] into Maxwell's equations

$$\left[\partial_z^2+\frac{\omega^2}{c^2}\right]\delta\hat{A}_\pm(z)=-\frac{4\pi}{c}\delta\hat{J}_\pm(z)\ ,\quad \partial_z\delta\hat{\phi}(z)=\frac{8\pi i}{\omega}\delta\hat{J}_z(z)\ . \tag{20}$$

This results in a set of three coupled equations for the initial field amplitudes

$$\Lambda_\pm(k\mp k_w,\omega)\delta\hat{A}_\pm(0)+\tfrac{1}{2}a_w\frac{c^2k^2}{\omega^2}\chi_a(k,\omega)\delta\hat{\phi}(0)=0\ , \tag{21}$$

$$[1+\chi(k,\omega)]\delta\hat{\phi}(0)+a_w\frac{k_w}{k}[\delta\hat{A}_+(0)\sigma_+(k-k_w,\omega)+\delta\hat{A}_-(0)\sigma_-(k+k_w,\omega)]=0\ ,$$

where the wavelength matching conditions imply that $k_\pm=k\mp k_w$, and

$$\Lambda_\pm(k_\pm,\omega)\equiv 1-\frac{c^2k_\pm^2}{\omega^2}-\frac{\omega_b^2}{\omega^2}\left\langle\frac{p}{\gamma p_z}\frac{\omega-k_\pm v_{||}}{\omega\mp\Omega_0-k_\pm v_{||}}\right\rangle-\frac{\omega_b^2}{2\omega^2}a_w^2S_\pm(k_\pm,\omega) \tag{22}$$

describes the dispersion properties of the pure electromagnetic modes in the combined wiggler and axial guide fields. The dispersion equation itself is found by setting the determinant of the matrix of coefficients of Eqs. (21) to zero, which yields

$$1+\chi(k,\omega)=\frac{a_w^2}{2}\frac{k_w}{k}\frac{c^2k^2}{\omega^2}\chi_a(k,\omega)\left[\frac{\sigma_+(k-k_w,\omega)}{\Lambda_+(k-k_w,\omega)}+\frac{\sigma_-(k+k_w,\omega)}{\Lambda_-(k+k_w,\omega)}\right]\ . \tag{23}$$

It is evident that Eq. (23) describes the coupling between the electrostatic beam mode with each of the electromagnetic modes.

In the interest of analytic tractability, we shall now assume that the electron beam is sufficiently cold that a monoenergetic distribution of the form

$$G_b(p)=\frac{p_z}{p}\delta(p-p_0) \tag{24}$$

can be employed. As mentioned previously, this is generally valid as long as the momentum spread $\Delta p \ll p_0/N$. Combination of (23) and (24) yields a dispersion equation of the form

$$(\omega-kv_{||})^2-\kappa^2v_{||}^2=-\frac{\beta_w^2}{2}\frac{\omega_b^2}{\gamma}\left[\frac{\alpha_+(k-k_w,\omega)}{\epsilon_+(k-k_w,\omega)}+\frac{\alpha_-(k+k_w,\omega)}{\epsilon_-(k+k_w,\omega)}\right] \tag{25}$$

to second order in the wiggler amplitude, where all orbit quantities (i.e., $v_{||}$, γ_z, β_w, etc.) are computed using p_0,

$$\kappa^2v_{||}^2\equiv\frac{\omega_b^2}{\gamma\gamma_z^2}\Phi\ , \tag{26}$$

$$\epsilon_\pm(k_\pm,\omega)\equiv 1\frac{\omega_b^2(\omega-k_\pm v_{||})}{\gamma(\omega^2-k_\pm^2c^2)(\omega\mp\Omega_0-k_\pm v_{||})}\ , \tag{27}$$

and

$$\alpha_\pm(k\mp k_w,\omega)\equiv\frac{1}{\omega^2-(k\mp k_w)^2c^2}$$
$$\times\left[\beta_{||}^2(\omega^2-k^2c^2-\omega_b^2/\gamma)+\frac{\omega_b^2}{\gamma}\beta_{||}^2(\omega-kv_{||})^{-2}\right.$$
$$\left.\times[(1-\Psi^2)(kc-\omega v_{||}/c)^2+\gamma_z^{-2}(1-\Phi)(\omega^2-k^2c^2)]\right.$$

$$+\frac{\omega_b^2}{\gamma\omega}\frac{\Omega_0}{k_w v_{||}-\Omega_0}\beta_{||}(kc-\omega v_{||}/c)\Psi\left[\frac{\omega\mp k_w v_{||}}{\omega-kv_{||}}-\frac{\omega}{\omega\mp\Omega_0-(k\mp k_w)v_{||}}\right]$$

$$+\frac{\Omega_0}{k_w v_{||}-\Omega_0}[(\omega-kv_{||})^2-\kappa^2 v_{||}^2]\left[\frac{3\omega\mp k_w v_{||}}{\omega-kv_{||}}-\frac{\omega\mp\Omega_0\pm k_w v_{||}}{\omega\mp\Omega_0-(k\mp k_w)v_{||}}\right]$$

$$-\gamma_z^{-2}(1-\Phi)[(\omega-kv_{||})^2-\kappa^2 v_{||}^2]\frac{\omega}{\omega-kv_{||}}\left[\frac{\omega-2kv_{||}}{\omega-kv_{||}}+\frac{2\Omega_0}{k_w v_{||}-\Omega_0}\right]\Bigg]. \tag{28}$$

In addition, we have defined

$$\Phi\equiv 1-\frac{\Omega_0\beta_w^2\gamma_z^2}{(1+\beta_w^2)\Omega_0-k_w v_{||}} \tag{29}$$

and

$$\Psi\equiv 1-\frac{\Omega_0}{\beta_{||}(kc-\omega v_{||}/c)}\frac{(1+\beta_w^2)k_w v_{||}-\omega}{(1+\beta_w^2)\Omega_0-k_w v_{||}}\,. \tag{30}$$

In Eq. (25), $\epsilon_{\pm}(k\mp k_w,\omega)$ describes the circularly polarized electromagnetic modes in the absence of the wiggler, and the left-hand side describes the electrostatic beam modes. Observe, however, that the presence of the wiggler modifies the natural electrostatic response frequency by a factor of Φ defined in (29).

The wiggler field, therefore, provides a coupling between the space-charge wave and either polarization state of the electromagnetic wave. We choose, without loss of generality, to focus on the coupling with the $\delta\hat{A}_+$ mode. As a consequence, we shall assume that $|\epsilon_+(k-k_w,\omega)| \ll |\epsilon_-(k+k_w,\omega)|$ and neglect the term in $\epsilon_-^{-1}(k+k_w,\omega)$ in (25). If we assume in addition that $\omega_b^2/\gamma\omega^2 \ll 1$, then the dispersion equation can be cast into the substantially simpler form

$$[(\omega-kv_{||})^2-\kappa^2 v_{||}^2]\left[\omega^2-k_+^2c^2-\frac{\omega_b^2(\omega-k_+v_{||})}{\gamma(\omega-\Omega_0-k_+v_{||})}\right]$$

$$\simeq-\frac{\beta_w^2}{2}\frac{\omega_b^2}{\gamma}\left[\beta_{||}^2\left[\omega^2-k^2c^2-\frac{\omega_b^2(\omega-k_+v_{||})}{\gamma(\omega-\Omega_0-k_+v_{||})}\right]+\gamma_z^{-2}\omega^2(1-\Phi)+\omega\Omega_0\frac{\omega-kv_{||}}{\omega-\Omega_0-k_+v_{||}}\right], \tag{31}$$

where we have written $k_+=k-k_w$ for simplicity. Peak gain in (31) can be expected to occur near the intersections of the electrostatic and electromagnetic dispersion curves. A schematic representation of the dispersion relation is shown in Fig. 2 for $\Omega_0>\omega_b/\gamma^{1/2}$. Evidently, high-frequency interactions with the electrostatic beam mode can occur only in the positive ω and k_+ quadrant when $v_{||}>0$, and we shall restrict the analysis to this regime. It should be observed that the slope of the space-charge modes ($\omega=k_+v_{||}+k_w v_{||}\pm\kappa v_{||}$) is identical to the pure cyclotron mode ($\omega=k_+v_{||}+\Omega_0$), and the relative magnitudes of the $k_+=0$ intercepts of these curves determine which branch of the electromagnetic dispersion curve participates in the interaction. This point will be discussed in more depth at a later stage of the analysis.

The dispersion equation represented by (31) is a fifth-degree polynomial in k. If we make the restriction that $k_+>0$, then (31) can be reduced to the following quartic equation:

$$\left[k-\frac{\omega}{v_{||}}-\kappa\right]\left[k-\frac{\omega}{v_{||}}+\kappa\right](k-k_w-K_+)(k-k_w-K_-)$$

$$\simeq-\frac{\beta_w^2}{4}\xi^2k_w^2\frac{\omega}{Kc}\beta_{||}^{-1}\left[\frac{\omega}{\gamma_z^2 v_{||}}\Phi\left[k-k_w-\frac{\omega-\Omega_0}{v_{||}}\right]-\frac{\Omega_0}{v_{||}}\left[k-\frac{\omega}{v_{||}}\right]\right], \tag{32}$$

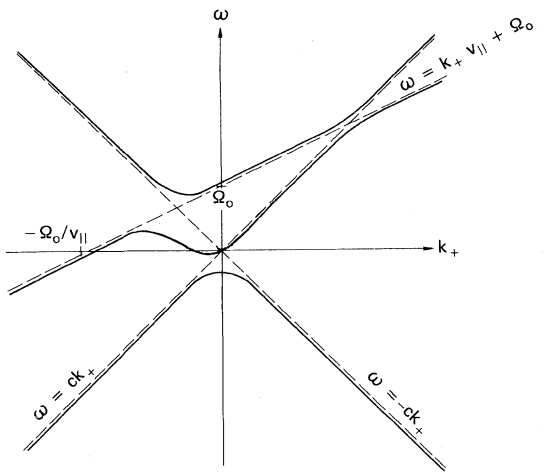

FIG. 2. Schematic representation of the dispersion curves for the $\delta\hat{A}_+$ mode showing the passive interaction between the cyclotron and the pure electromagnetic mode at $\omega \simeq (1-\beta_{||})^{-1}\Omega_0$.

where $\xi=\omega_b/\gamma^{1/2}ck_w$ is the beam strength, $c^2K^2\equiv\omega^2-\omega_b^2/\gamma$,

$$K_\pm \equiv \frac{1}{2}\left[K+\frac{\omega-\Omega_0}{v_{||}}\right] \pm \frac{1}{2}\left[\Delta K^2+2\xi^2k_w^2\frac{\Omega_0}{Kv_{||}}\right]^{1/2}, \tag{33}$$

and $\Delta K\equiv K-(\omega-\Omega_0)/v_{||}$. It is clear that the nature of the interaction is strongly dependent upon the sign of Φ, which affects the natural electrostatic response frequency of the plasma as well as mediating the ponderomotive force.[2] In the limit as $B_0\to 0$, Φ approaches unity and (32) reduces to the well-known results in the limit of zero axial field.[20–22] The behavior of Φ when the guide field is finite, however, is strongly dependent on the type of orbit under consideration. The variation of Φ with β_0 is shown in Fig. 3 for the parameters used to generate the orbits in Fig. 1. As shown in the figure, $\Phi\geq 1$ for group I orbits and contains a singularity when $\Omega_0(1+\beta_w^2)=k_wv_{||}$ which is the orbital stability boundary. In the case of group II orbits the magnitude of Φ is, typically, less than or of the order of unity, but Φ is negative for axial guide fields less than a critical magnitude given by $[1+\beta_w^2(1-\gamma_z^2)]\Omega_0=k_wv_{||}$. As B_0 increases beyond this critical value Φ approaches unity; however, it should be noted that β_w decreases monotonically with increasing B_0 in this regime. In either case in which $\Phi>0$, the interaction is basically one in which a positive-energy electromagnetic wave is coupled to a negative-energy space-charge wave by the action of the wiggler. Neither wave is intrinsically unstable and growth occurs when the wiggler amplitude is above threshold. However, when Φ is less than zero, κ is imaginary and the space-charge waves, themselves, comprise a complex-conjugate pair $\omega=kv_{||}\pm i\,|\,\kappa\,|\,v_{||}$, one of which is unstable. As a result, we shall distinguish between these two possibilities and treat the solution to the dispersion equation when Φ is positive and negative separately.

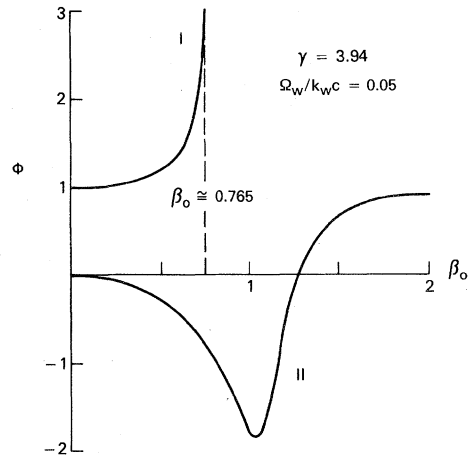

FIG. 3. Graph of Φ vs β_0 for both group I and group II orbits for a beam energy of 1.5 MeV and a wiggler amplitude and period such that $\Omega_w/k_wc=0.05$.

A. $\Phi>0$

In this regime we observe that the orbital stability criterion implies that

$$k_wv_{||}>\Omega_0\left[1+\left[\frac{B_w}{B_0}\right]^{2/3}\right] \tag{34}$$

for group I orbits, and the requirement that Φ be positive leads to the condition that

$$k_wv_{||}<\Omega_0\left[1-(\gamma_z^2-1)^{1/3}\left[\frac{B_w}{B_0}\right]^{2/3}\right] \tag{35}$$

for group II orbits. As a consequence, the intersection between the space-charge and electromagnetic modes occurs at frequencies greater (less) than $\Omega_0(1-\beta_{||})^{-1}$ for group I (II) orbits when $\kappa v_{||}\ll|\,k_wv_{||}-\Omega_0\,|$. This condition is satisfied as long as $\Phi<\gamma_z\xi^{-1}(B_w/B_0)^{2/3}$ and, since $\xi\ll 1$ is implicitly assumed in order to neglect self-field effects, is a relatively weak constraint. A schematic representation of the interaction is shown in Figs. 4(a) and 4(b) for group I and II orbits in which we plot ω versus k_+ and the dotted line represents

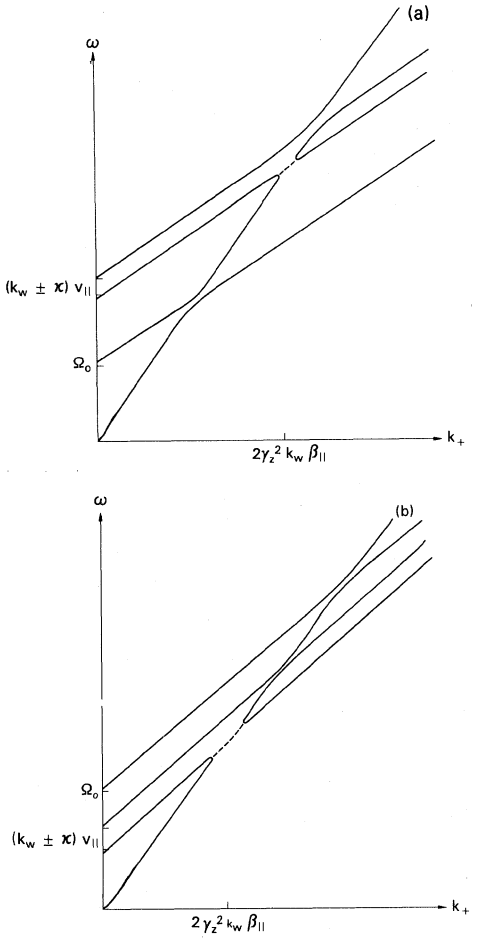

FIG. 4. Schematic representation of the interaction for group I (a) and group II (b) orbits when $\Phi>0$. Dotted line denotes complex-conjugate roots.

complex-conjugate roots. It is the lower (i.e., $\omega=kv_{||}-\kappa v_{||}$) space-charge mode which produces the active coupling and wave growth since this is the negative-energy mode. We note that from (34) and (35), the intersections are not close to the cyclotron line and occur approximately for $\omega\simeq ck_+\simeq(k_++k_w)v_{||}$. This is the well-known free-electron laser resonance at $k_+\simeq 2\gamma_z^2 k_w\beta_{||}$.

If the beam strength parameter is sufficiently small that $\xi\ll\gamma_z(B_w/B_0)^{2/3}$ and $\gamma_z(B_w/B_0)^{2/3}\times\Phi^{1/2}$, then the cyclotron resonance effects can be neglected and the dispersion equation reduces to the cubic

$$\delta k(\delta k+2\kappa)(\delta k-\Delta k)\simeq-\frac{\beta_w^2}{4}\xi^2 k_w^2\beta_{||}^{-1}\Phi\frac{\omega}{\gamma_z^2 v_{||}}\ , \tag{36}$$

where we have chosen $\delta k\equiv k-\omega/v_{||}-\kappa$, and $\Delta k\equiv k_w+K-\omega/v_{||}-\kappa$ is the frequency mismatch parameter. Equation (36) reduces to the result found by Sprangle and Smith[20] in the limit as $B_0\to 0$, and corresponds to the limit discussed by Friedland and Fruchtman.[13]

The single-particle or "strong-pump" regime occurs when $|\delta k|\gg|2\kappa|$. In this regime, (36) can be approximated by

$$\delta k^2(\delta k-\Delta k)\simeq-\frac{\beta_w^2}{4}\xi^2 k_w\beta_{||}^{-1}\Phi\frac{\omega}{\gamma_z^2 v_{||}}\ . \tag{37}$$

Peak growth occurs when $\Delta k\simeq 0$, for which the complex roots are

$$(\delta k)_{\max}\simeq\tfrac{1}{2}(1\pm i\sqrt{3})\left[\frac{\beta_w^2}{2}\xi^2\beta_{||}^{-1}\Phi\right]^{1/3}k_w\ . \tag{38}$$

Therefore, self-consistency imposes the requirement that

$$\kappa\ll\tfrac{1}{16}\beta_w^2\gamma_z^2\beta_{||}k_w \tag{39}$$

in order for Eq. (37) to be valid. It is important to recognize that in this regime the coupling between the electrostatic beam mode and the $\delta\hat{A}_+$ mode is relatively unimportant, and the strength of the pump and ponderomotive potential completely dominate the interaction. Because of this, (37) can be recovered in a much more direct manner by ignoring the space-charge potential in (21) and setting $\Lambda_+(k-k_w,\omega)=0$.

In the opposite, or space-charge dominated (or stimulated Raman scattering), regime, $|\delta k|\ll|2\kappa|$ and space-charge effects are predominant. Here, the dispersion equation is of the form

$$\delta k^2-\Delta k\delta k+\frac{\beta_w^2}{4}\gamma_z^2\beta_{||}\kappa k_w\simeq 0\ , \tag{40}$$

which has the solutions

$$\delta k\simeq\tfrac{1}{2}\Delta k\pm\tfrac{1}{2}(\Delta k^2-\beta_w^2\gamma_z^2\beta_{||}\kappa k_w)^{1/2}\ . \tag{41}$$

Peak gain is found for $\Delta k\simeq 0$ in this regime as well and is

$$(\delta k)_{\max}\simeq\tfrac{1}{2}i\beta_w\gamma_z k_w\left[\beta_{||}\frac{\kappa}{k_w}\right]^{1/2}\ . \tag{42}$$

The Raman regime, therefore, occurs when

$$\kappa\gg\tfrac{1}{8}\beta_w^2\gamma_z^2\beta_{||}k_w\ , \tag{43}$$

and requires relatively large beam currents.

B. $\Phi<0$

As mentioned previously, the space-charge waves are intrinsically unstable in this regime and a relatively broadhanded spectrum of excited electrostatic-electromagnetic waves is expected to occur. In addition, since we are dealing with group II orbits

$$\Omega_0\left[1-(\gamma_z^2-1)^{1/3}\left[\frac{B_w}{B_0}\right]^{2/3}\right]<k_w v_{||}<\Omega_0\ , \tag{44}$$

and the possibility of a cyclotron mode interaction exists when $\gamma_z^2-1\ll(B_0/B_w)^2$.

In the high frequency $\omega\gg(1-\beta_{||})^{-1}\Omega_0$ and high $k\gg k_w$ regime, the space-charge waves are characterized by frequencies $\omega\ll ck_+$, and the cyclotron resonance contributions can be ignored when

$$\xi\ll\frac{\omega}{ck_w}\,|\,\Phi\,|^{1/2}\beta_{||}\gamma_z^{-1}(\gamma_z^2-1)^{1/3}\left[\frac{B_w}{B_0}\right]^{2/3}\ . \tag{45}$$

In this regime we recover the cubic dispersion Eq. (36) found earlier (when $\Phi>0$). For frequencies such that $|\,\Delta k\,|\ll\delta k$ the free-electron laser solutions are obtained; however, for high-frequency space-charge modes $|\,\Delta k\,|\simeq\omega(1-\beta_{||})/v_{||}\gg|\,\delta k\,|$. For these waves, the dispersion equation can be approximated by the quadratic

$$k^2-2\frac{\omega}{v_{||}}k+\frac{\omega^2}{v_{||}^2}+|\,\kappa\,|^2\left[1-\frac{\beta_w^2}{4}\beta_{||}\gamma_z^2(1+\beta_{||})\right]\simeq 0\ , \tag{46}$$

which has been expressed in terms of k rather than δk for convenience. The solution

$$k\simeq\frac{\omega}{v_{||}}\pm i\,|\,\kappa\,|\left[1-\frac{\beta_w^2}{4}\beta_{||}\gamma_z^2(1+\beta_{||})\right]^{1/2} \tag{47}$$

is obviously a modified space-charge wave. It should be observed that the presence of the wiggler acts as a stabilizing influence, and for sufficiently strong pumps [i.e., $\beta_w^2\beta_{||}\gamma_z^2(1+\beta_{||})>4$] the mode is stable.

In the opposite limit in which $\omega\ll(1-\beta_{||})^{-1}\Omega_0$, it is more difficult to satisfy condition (45), and the cyclotron resonance is of greater importance. This regime will be discussed in depth in Sec. IV in the context of a complete numerical solution of the dispersion equation.

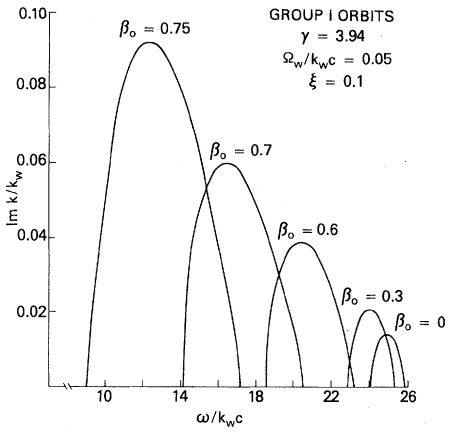

FIG. 5. Graph of $\mathrm{Im}k/k_w$ vs ω/k_wc for group I orbits.

IV. NUMERICAL ANALYSIS

In this section, we conduct an extensive numerical analysis of the quartic dispersion Eq. (32) for a beam characterized by $\gamma=3.94$ (1.5 MeV) and $\xi=0.1$, and a wiggler such that $\Omega_w/k_wc=0.05$. Our procedure is to solve (32) for a wide range of axial field strengths in the vicinity of $\Omega_0\simeq k_wc$ by self-consistently calculating $v_{||}$ for each case and for both types of stable trajectory. As in Sec. III, we distinguish between the regimes for which Φ is positive and negative.

In the limits in which Φ is positive, the dispersion properties of (32) are qualitatively represented

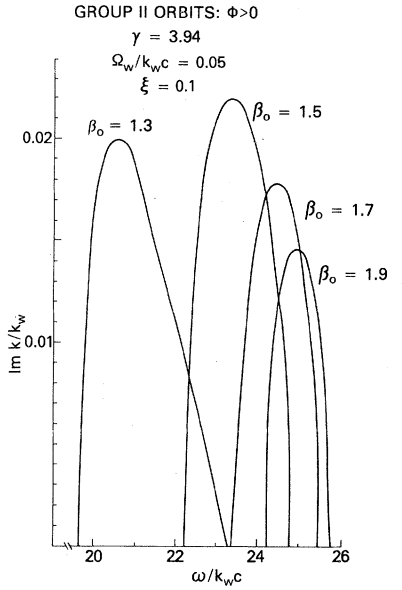

FIG. 6. Graph of $\mathrm{Im}k/k_w$ vs ω/k_w for group II orbits ($\Phi>0$).

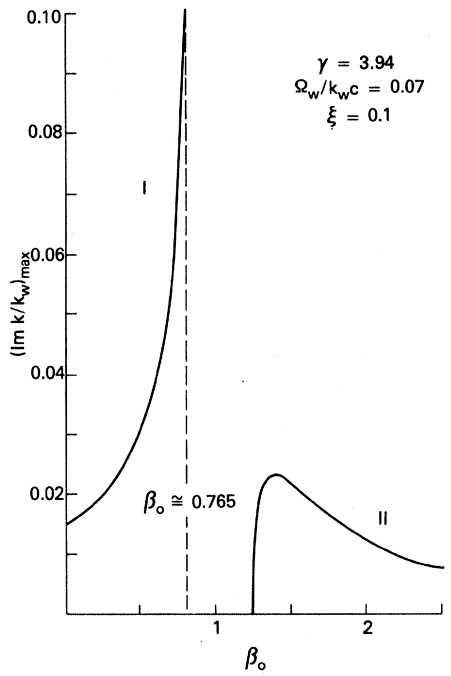

FIG. 7. Graph of $(\mathrm{Im}k/k_w)_{\max}$ as a function of the axial guide field for group I and group II ($\Phi > 0$) orbits.

in Fig. 4 for orbits in groups I and II. The growth rates (Im k/k_w) are plotted versus frequency for several appropriate values of β_0 in Figs. 5 and 6 for the two types of trajectory. Instability is found to occur for $\omega \simeq (1-\beta_{\|})^{-1} k_w v_{\|}$ which corresponds to the well-known free-electron laser resonance condition. The observation of decreasing (increasing) frequencies of instability with increasing axial field for group I (II) orbits can, therefore, be explained by examination of Fig. 1 in which it is seen that $v_{\|}$ decreases (increases) with increasing β_0.

The behavior of the peak growth rates for the two classes of orbits can also be readily explained. As shown in Fig. 7, the peak growth rate for group I orbits is a monotonically increasing function of B_0 up to the singularity at the orbital stability boundary (at $\beta_0 \simeq 0.765$ for this choice of parameters). This behavior is due to increases in both β_w and Φ with the axial field which results in increases in the effects of both the electrostatic/electromagnetic coupling and the ponderomotive potential. Observe, however, that the singularity is due solely to the character of Φ since β_w is everywhere finite. The scaling of the maximum growth rate with β_0 is also shown in Fig. 7 for group II trajectories. In this case, however, Φ is bounded by unity and increases monotonically from zero (at $\beta_0 \simeq 1.25$) with increasing axial fields. In addition, β_w decreases monotonically to zero with increasing B_0 for group II orbits since $\lim_{B_0 \to \infty} \beta_w = B_w/B_0$. As a consequence, the peak growth can be expected to initially increase from zero at $\beta_0 \simeq 1.25$, and to decrease again slowly to zero as the axial field becomes large. This behavior for the growth rates of each class of orbit is in qualitative agreement with that found previously in the context of a low gain theory.[15] Finally, since it is our intention to treat the collective re-

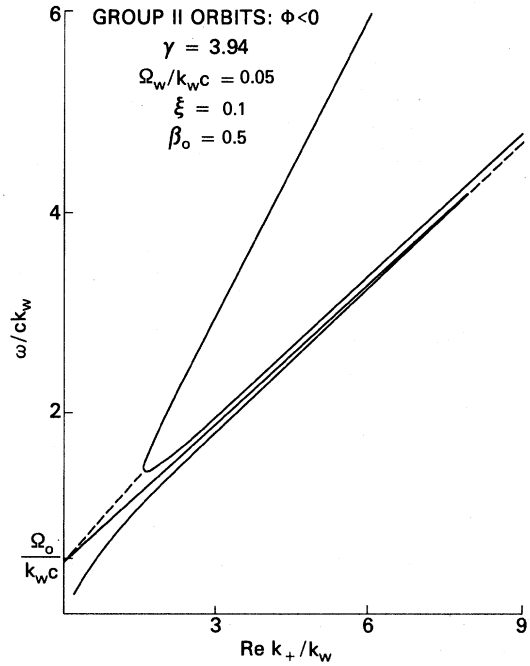

FIG. 8. Graph of ω/ck_w vs $\mathrm{Re}k_+/k_w$ for group II orbits ($\Phi < 0$) and $\beta_0 = 0.5$.

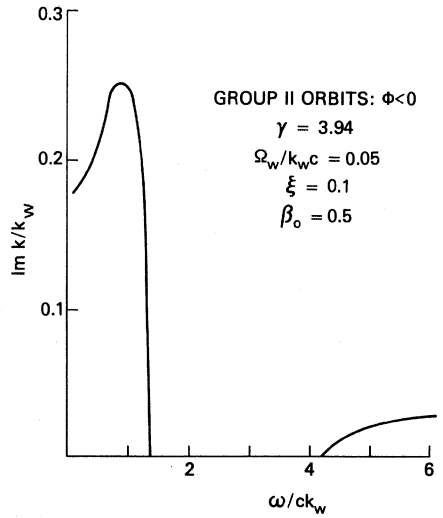

FIG. 9. Graph of $\mathrm{Im}k/k_w$ vs ω/ck_w for group II ($\Phi < 0$) orbits and $\beta_0 = 0.5$.

gime, the parameters have been chosen to correspond to the space-charge dominated limit discussed in Sec. III and the numerical results for the peak gain can be recovered from Eq. (40) to within an error of a few percent.

Some care must be taken in the characterization of the dispersion properties of (32) when $\Phi<0$. For low axial fields ($\beta_0 \lesssim 0.7$ for the parameters under consideration) both $v_{||}$ and $|\Phi|$ are low and condition (43) is not well satisfied when $\omega<(1-\beta_{||})^{-1}\Omega_0$. This regime is illustrated in Figs. 8 and 9 in which we plot ω/ck_w versus $\mathrm{Re}k_+/k_w$ and $\mathrm{Im}k/k_w$ versus ω/ck_w, respectively, for $\beta_0=0.5$. The dashed line in Fig. 8 corresponds to complex-conjugate roots. Evidently, two instability regimes exist. At high frequencies, the modified space-charge wave discussed in Sec. III B is obtained with an asymptotic value (i.e., high-ω limit of $\mathrm{Im}k/k_w$) which agrees to within 1% of the predicted value in Eq. (45). The instability found at lower frequencies is difficult to treat analytically, and corresponds to a modified cyclotron mode.

For higher axial fields ($\beta_0 \gtrsim 0.7$), the character of the unstable modes is altered. As shown in Fig. 10, in which we plot ω/ck_w versus $\mathrm{Re}k_+/k_w$ for $\beta_0=1$, there are still two unstable regimes. While the higher frequency regime corresponds to the modified space-charge mode in this case as well, the lower frequency instability requires some discussion. The growth rate in this regime is plotted as a function of frequency in Fig. 11 for $\beta_0=0.8$, 1, and

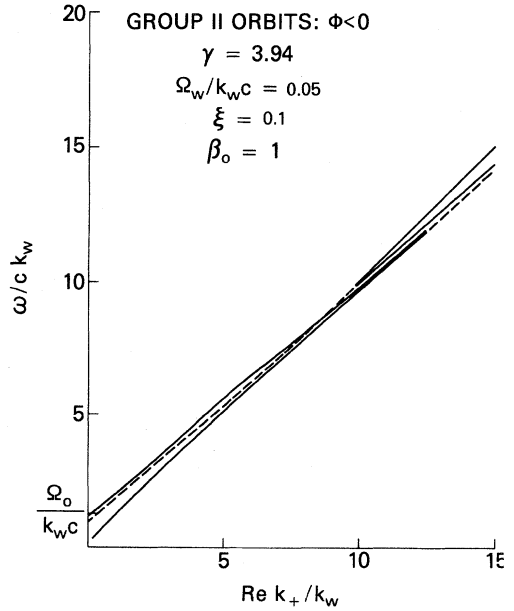

FIG. 10. Graph of ω/ck_w vs $\mathrm{Re}k_+/k_w$ for group II ($\Phi<0$) orbits and $\beta_0=1$.

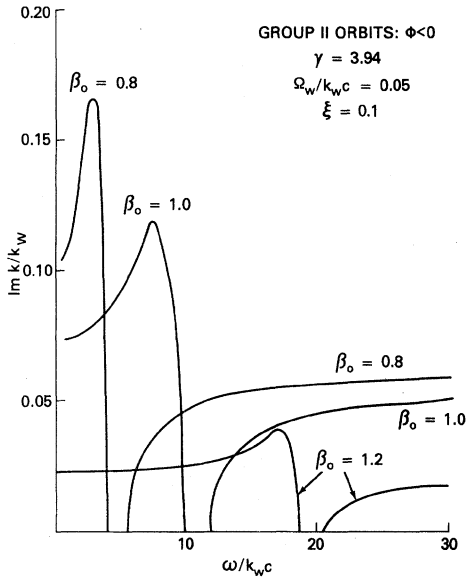

FIG. 11. Graph of $\mathrm{Im}k/k_w$ vs ω/ck_w for group II ($\Phi<0$) orbits and $\beta_0=0.8$, 1, and 1.2.

1.2. In each case, the peak in $\mathrm{Im}k/k_w$ observed for the lower frequency instability corresponds to the region shown in Fig. 10 in which the real part of the complex modes (dashed line) exceeds that of the waves which are purely real. Near the peak $\Delta k \simeq 0$, and the instability which results is a largely electromagnetic free-electron laser interaction which (for our choice of parameters) agrees to within a few percent of the analytic expression for the peak growth rate (40) in the collective, or stimulated Raman scattering, limit. As the frequency decreases, $|\Delta k|$ increases and the character of the instability becomes increasingly electrostatic and we find an unstable modified space-charge wave for frequencies $\omega \gtrsim \Omega_0$.

V. SUMMARY AND DISCUSSION

In this paper we have analyzed the linear growth rate in both the single-particle and collective regimes of operation of a free-electron laser configuration which contains a uniform axial guide field. The technique employed consists, essentially, of a Vlasov theory of the perturbations about constant-$v_{||}$ helical trajectories, and includes the effects of both stimulated Raman scattering with electrostatic beam modes and the effect of the ponderomotive potential due to the exited radiation. Analytic expressions for the growth rate in these two regimes are found and a comparison is made with a numerical solution of the full dispersion equation. Sub-

stantial agreement is found between the analytical and numerical treatments. In addition, substantial qualitative agreement also exists between the present work, which is in the high gain regime, and the small signal theories.[11,15]

The results indicate that substantial enhancements in the growth rate of the free-electron laser instability may be obtained by the inclusion of an axial guide field in which $\Omega_0 \simeq ck_w$, as a result of increases both in the transverse velocity and the ponderomotive potential. It should be pointed out, however, that the presence of the guide field also gives rise to instability in the electrostatic beam mode for group II orbits when $\Phi < 0$. Since this may have a degrading effect on beam quality and, in turn, on the operating efficiency, further study of this question is required.

A cyclotron mode interaction in the collective regime has been found only where the axial velocity and $|\Phi|$ are relatively small. However, two factors should be noted. The first is that our choice of equilibrium orbits (i.e., with $P_x = P_y = 0$) has intrinsically ignored the random (or Larmor) component of the transverse velocity which can be expected to be the primary source of a gyrotron type of instability. The second is our choice of an idealized magnetic field structure in which transverse gradients in the wiggler field have been neglected, which is valid only for orbits in which $k_w r \ll 1$. Since small $v_{\|}$ implies large transverse velocities and excursions from the axis of symmetry, the choice of an ideal wiggler ultimately breaks down in this limit.

ACKNOWLEDGMENTS

This work was supported, in part, under NAVAIR Contract No. WF32-389-592. In addition, support for several of us (E.H.J., B.L., and R.S.S.) was provided by the Conselho Nacional de Desenvolvimento Cientifico e Technologico and the Financiadora de Estudos e Projetos of Brazil.

*Permanent address: Science Applications, Inc., McLean, Va. 22102.

[1]D. B. McDermott, T. C. Marshall, S. P. Schlesinger, R. K. Parker, and V. L. Granatstein, Phys. Rev. Lett. 41, 1368 (1978).

[2]S. H. Gold, R. H. Jackson, R. K. Parker, H. P. Freund, V. L. Granatstein, P. C. Efthimion, M. Herndon, and A. K. Kinkead, in *Physics of Quantum Electronics* edited by S. F. Jacobs, H. S. Pilloff, M. Sargent, M. O. Scully, and R. Spitzer (Addison-Wesley, New York, 1982), Vol. 9.

[3]R. E. Shefer and G. Bekefi, Bull. Am. Phys. Soc. 26, 846 (1981).

[4]C. W. Roberson, J. Pasour, F. Mako, R. Gilgenbach, and P. Sprangle, Bull. Am. Phys. Soc. 26, 1016 (1981).

[5]K. Felch, L. Vallier, and J. M. Buzzi, Bull. Am. Phys. Soc. 26, 945 (1981).

[6]L. R. Elias, W. M. Fairbank, J. M. J. Madey, H. A. Schwettman, and T. I. Smith, Phys. Rev. Lett. 36, 717 (1976).

[7]D. A. G. Deacon, L. R. Elias, J. M. J. Madey, G. J. Ramian, H. A. Schwettman, and T. I. Smith, Phys. Rev. Lett. 38, 892 (1977).

[8]H. Boehmer, M. Z. Caponi, J. Edighoffer, S. Fornaca, J. Munch, G. Neil, B. Saur, and C. Shih, Bull. Am. Phys. Soc. 26, 853 (1981).

[9]P. Sprangle, V. L. Granatstein, and L. Baker, Phys. Rev. A 12, 1697 (1975).

[10]T. Kwan and J. M. Dawson, Phys. Fluids 22, 1089 (1979).

[11]L. Friedland and J. L. Hirshfield, Phys. Rev. Lett. 44, 1456 (1980).

[12]I. B. Bernstein and L. Friedland, Phys. Rev. A 23, 816 (1981).

[13]L. Friedland and A. Fruchtman, Bull. Am. Phys. Soc. 26, 1016 (1981).

[14]M. Z. Caponi, J. Munch, and M. Boehmer, in *Free Electron Generators of Coherent Radiation,* edited by S. F. Jacobs, H. S. Pilloff, M. Sargent, M. O. Scully, and R. Spitzer (Addison-Wesley, New York, 1980), p. 523.

[15]H. P. Freund, P. Sprangle, D. Dillenburg, E. H. da Jornada, B. Liberman, and R. S. Schneider, Phys. Rev. A 24, 1965 (1981).

[16]S. Johnston, in *Physics of Quantum Electronics,* Ref. 2, Vol. 9.

[17]L. Friedland, Phys. Fluids 23, 2376 (1980).

[18]H. P. Freund and A. T. Drobot, Phys. Fluids 25, 736 (1982).

[19]P. Diament, Phys. Rev. A 23, 2537 (1981).

[20]P. Sprangle and R. A. Smith, Phys. Rev. A 21, 293 (1980).

[21]I. B. Bernstein and J. L. Hirshfield, Phys. Rev. A 20, 1661 (1979).

[22]R. C. Davidson and H. S. Uhm, Phys. Fluids 23, 2076 (1980).